International Journal on Electrical Engineering and Informatics - Volume 15, Number 3, September 2023

Multi-Objective Optimization to find the Location and Power Capacity of DC Traction Substations to supply the MRT System with Multi-Train

Tahan Lumban Tobing[1.2], Tri Desmana Rachmidha[1], Hilwadi Hindersah[1] and Suwarno[1]

[1]Departement of Electrical Engineering, Universitas Kristen Indonesia, Jakarta, Indonesia.
[2]School of Electrical Engineering and Informatics, Institute Technology of Bandung, Bandung, Indonesia

Abstract: Finding the optimal location and power capacity of traction substations is a problem in the design of DC electric power supply systems for trains. The proposed method uses evolutionary multi-objective optimization (EMO) to find the solution. By using two optimization steps: firstly, finding the Pareto optimal solutions with NSGA-ii method, and secondly, selecting from the Pareto optimal solutions by using higher-level information to obtain the best solution. The method is used to optimize 15 kilometer (km) railway power supply systems with three or four traction substations. The load sharing between the traction substations is almost the same as the minimum power capacity. Therefore, the single best solution is obtained, showing that the minimum solution requirements for the location and power capacity of the traction substations are met.

Keyword: EMO Optimization, Pareto Optimal, Traction Substation, Peak Demand, Energy Needs.

1. Introduction

Many large cities worldwide have used and are building rail-based electric mass transportation due to the efficiency of energy consumption per passenger and pollution cleanliness compared to bus or tram-based mass transportation [1] [2]. The electrical power supply system for mass rapid transit (MRT) trains is designed to meet the requirements of sustainable development, be environmentally friendly, and be energy efficient [3]. Research on energy savings and efficient use of the train's electrical power supply system has been conducted for a long time. [4] proposed several important formulas for energy conservation in train DC power supply systems to achieve an economically distributed system, including determining the ideal distance between traction substations affected by the maximum voltage drop and setting the allowable overload current of the track feeder circuit breaker (in the worst case, a short circuit should always be sufficient to trip the circuit breaker). [5] If the number of passenger stations per traction substation and the traffic density are low, then for the lowest capacity requirement, the traction substation should be located midway between adjacent stations. [6] The assumptions for calculating the distance between substations are that the electric current used by all trains is the same and that the distance between trains is the same [7].

The use of optimization methods in the calculation of train DC power supply systems seems to have started in 2008 [8]. The selection of the numbers, the capacity and the distance between traction substations to minimizing the power losses of the railway power supply system. Then the optimization using the genetic algorithm method was carried out [9]. A method for optimizing the location of rectifier substations based on multi-objective optimization with weighting factors, resulting in a single objective function or single objective genetic optimization that is able to calculate energy requirements and peak power demand to be optimized. Whereby, the application of the method was in Line 4 of Metro Sao Paolo Brazil. Then the work of [10], a single objective Genetic algorithm meta-heuristic optimization method [11] with peak demand objective function and fitness function is the DC power flow model. The optimization method developed is sufficient for simplified cases of DC power system design, so the convex optimization problem applies. In this paper, the use of the Evolutionary Multi-Objective Optimization (EMO) optimization method is developed for optimization cases where the convex condition no longer applies. Then the proposed methods are used to study the railway power supply system for the Jakarta MRT.

The sequencing of this paper is as follows: the Problem is divided into three parts: the mechanical characteristics of the train, the power flow of the train system, and the multi-objective function

Received: June 8th, 2023. Accepted: September 15th, 2023
DOI: 10.15676/ijeei.2023.15.3.8

problem. After that, the evolutionary multi-objective optimization method is applied to find the optimal position and nominal power of direct current traction substations. Then, the results with the EMO method are discussed and compared with the single objective genetic algorithm method. Finally, the paper concludes.

2. Problem

A. MRT Train Movement and Energy Consumption Model

The mechanical power of the train is the power used by the train to move or to create a drag force on the train [12]. An important component in this modelling is the weight of the train; this affects the drag force on the train, which determines the movement of the train [13] [14]. Based on Newton’s second equation, the drag force is directly proportional to the mass of the train and the acceleration of the train [15]. The four drag forces, for acceleration, inclined plane, friction and wind resistance, and bending resistance [16], are summed to give the total drag force, which is the total drag force needed to produce motion in the train.

The total tractive force required to move the train is generated by the motors on the train. The motor’s torque through the motor pinion drives the gears on the drive wheel shaft of the car. The relationship between motor torque and tractive effort can be explained by the fact that the Power output to the train wheels is equal to the efficiency of the Power input to the motor pinion. The pulling force of the train is the motor efficiency constant times the motor torque and gamma divided by the train radius and gravity constant, where Gamma is the ratio of pinion speed to wheel speed and the radius of the train wheel in meters, and the motor efficiency constant is the efficiency of the transmission from the motor to the train wheel drive shaft [17]. So, the mechanical Power of a train can be obtained [18]

$$P = \frac{1000}{3600}\frac{F_t v}{\eta}[watts] \tag{1}$$

where F_t is the total pulling force *kgf*, v is the train speed *km/h*, η is the motor efficiency. In this way, the required energy is derived by finding the average power of the motor multiplied by time. The movement of the train is determined by the pulling force and weight of the train interacting between the wheels and the rail road tracks through a certain area of contact. This phenomenon is called adhesion and has three states: slip, perfect rolling, and skidding.

The speed curve as a function of time so that the relationship between the electrical power required and the time or position of the train can be obtained. The speed curve as a function of time is approximated as a quadrilateral, where the acceleration time, the deceleration time, and the deceleration time are given, as well as the angle at the start point of acceleration and the angle at the end point of deceleration. By analyzing the speed curve against time, the speed after the acceleration action and the speed at the deceleration action are obtained, of course, if the acceleration time and the glide time and the deceleration time and vice versa are known. This is used in the movement of trains from one passenger station to another in the simulation. On a route, the average speed and the planned speed are required. The average speed calculation is the distance travelled divided by the time taken. The calculation for the planned speed is the journey time plus the stopping time at the passenger station.

B. Power Flow Model of the DC Electrical Power Supply System

Electric trains are constantly moving along the tracks, so their position and load always vary with time [19]. This makes it difficult to model the load flow in the direct case, where the load varies with time and position. Using the principle [20] that changes in load characteristics in a power flow model do not occur in a short time, so that there are no electrical transients, a power flow model can be configured at any time, consisting of all trains, traction substations, power supply cables, and earth. This creates a load flow circuit at each step of the simulator, taking snapshots of the train’s position relative to the traction substations and other trains. In this study, a power flow model of a DC electrical power supply sys- tem for trains [21], taking into account the rail potential, is presented.

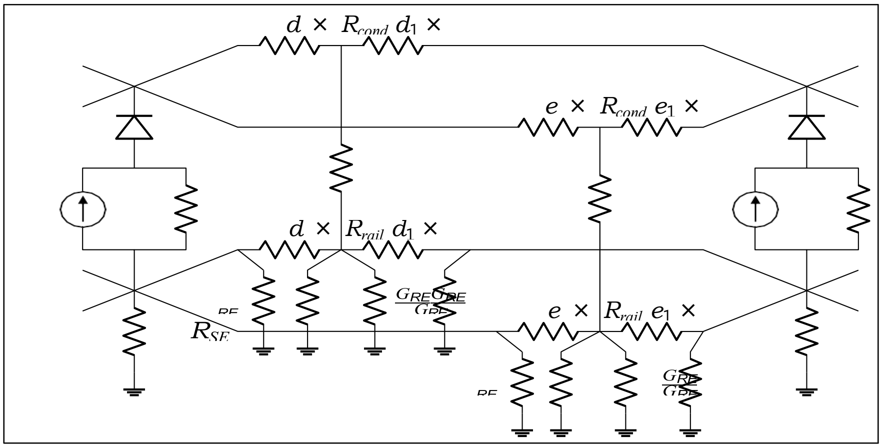

Figure 1. Train Power Flow Model Diagram

Thus, the power flow model is used to explain the voltage at the traction substation, the voltage at the train, the power consumed by each substation, the rail potential [22], and the power loss. Supported by the train model as a conductance matrix that can be positive when requiring current and negative when providing current due to regenerative braking, as seen in figure (1). The power supply to the train is modelled as a conductance in the simulation calculation.

The figure (1) is converted into a mathematical description of power flow [23] with a single train motion model as follows:

$$[I] = [G].[V] \tag{2}$$

where I is the current matrix, G is the conductance matrix, and V is the voltage matrix of the whole power flow model. Then, if the transmission in figure (1) is called point p to point q, then equation (2) is developed for the conductance matrix element, which is the element that describes the resistance due to the distance between the traction substation and the following traction substation, or between the traction substation and the train and between the train and the train, where the element for resistance is on the supply conductor and the element for resistance is on the rail road. Therefore, equation (2) is also developed for conductance matrix elements, which are elements that describe the resistance in traction substations or trains. And also developed as a grounding element for rails to distant earth, so equation (2) was developed and translated for the current at the traction substation into the following algebraic equation,

$$\begin{aligned} I^C(i) &= \frac{1}{R_s}V^C(i) - \frac{1}{R_s}V^R(i) - \frac{1}{d\ x\ R_{cond}}V^C(i+1) - I_s \\ I^R(i) &= \frac{-1}{R_s}V^C(i) + (\frac{1}{R_s} + \frac{1}{R_{se}} + \frac{1}{2}G_{re})V^R(i) - \frac{1}{d\ x\ R_{rail}}V^R(i+1) + I_s \end{aligned} \tag{3}$$

where $I^C(i)$ is the current on the conductor of the i_{th} traction substation, $V^C(i)$ is the voltage on the conductor of the i_{th} traction substation, $V^R(i)$ is the voltage on the rail of the i_{th} traction substation, $V^C(i+1)$ is the voltage on the conductor of the $(i+1)_{th}$ traction substation, $I^R(i)$ is the current on the rail traction substation, $V^R(i+1)$ is the voltage on the rail of the i+1st traction substation. In addition to being developed for the traction substation, it is also developed for the current on the train as follows,

$$I^C_{tr}(i) = \frac{1}{R_{tr}}V^C_{tr}(i) - \frac{1}{R_{tr}}V^R_{tr}(i) - \frac{1}{d\ x\ R_{cond}}V^C(k) \tag{4}$$

$$I^R_{tr}(i) = \frac{-1}{R_{tr}}V^C_{tr}(i) + (\frac{1}{R_{tr}} + \frac{1}{2}G_{re})V^R_{tr}(i) - \frac{1}{d\ x\ R_{rail}}V^R(k)$$

where $I\frac{C}{tr}$ is the current on the conductor of the train, $I\frac{R}{tr}$ is the current on the rail of the train, $V\frac{C}{tr}$ is the conductor voltage of the train, $V\frac{R}{tr}$ is the rail voltage of the train, $V^c(k)$ is the conductor voltage of the kth traction substation, $V^R(k)$ is the rail voltage of the kth traction substation.

After explaining the components that combine to make equation (2), which describes the load flow equation at a given time that changes with time and train position, equation (1) is used to obtain the electrical power provided by all the traction substations. The largest amount of electric power during a train trip, or peak demand, can be formulated as follows:

$$Pmax(i) = \sup\{P(i)|P(0) \leq P(i) \leq P(tp)\}[kW] \quad (5)$$

where *sup* is the supremum function (largest value) of $P(i)$ provided that $P(i)$ is in one period of train travel (0 to t_p) and i is the i_{th} traction sub-station. And consequently, the electrical power of each traction substation at any given time, or the energy supplied by the traction substation can be calculated, as described by the following equation:

$$E = \sum_{j=1}^{m} \overline{P_j}\Delta t\,[kWh] \quad (6)$$

where $\overline{P_j}$ is the average power of the j_{th} traction substation, m is the number of traction substations, Δt is a specific time.

C. Multi-objective Problem

The difference in peak demand, equation (5), between traction substations in a certain period is summed up. Then the sum of the differences will be minimized so that the traction substations each bear almost the same peak demand over a certain period of time. So this affects the positions of each substation to approach the source of peak demand for each substation at a certain time. where, the positions of traction substations that are close to the source of peak demand for each substation at a certain time will change the values of the conductance matrix G in equation (2). Through equations (3) and (4), the changes in the position of the sub- station change the value of R_{cond} and R_{rail} and so on, thus changing the

$$f_1 = \sum_{i}^{n_{ss}}\sum_{j}^{n_{ss}}\left|D_{max_i} - D_{max_j}\right| \quad (7)$$

$$f_2 = \sum_{i}^{n_{ss}}\sum_{j}^{n_{ss}}\left|E_i - E_j\right|$$

subject to

$$x_{kl} \leq x_k \leq x_{ku}$$

$$x_{cl} \leq D_i \leq x_{cu}$$

where index:

$$i = 1\ to\ n_{ss}$$

$$j = 1 + 1\ to\ n_{ss}$$

$$k = 1\ to\ n_{ss}$$

$$l = lower$$

$$u = upper$$

conductance matrix G in equation (2). But the change in position of each substation is limited by the minimum distance criteria between traction substations. However, if the peak demand difference of each substation is close to the same at a certain time, the amount of energy required, equation (6) by each traction substation at a certain time will be higher, and vice versa [9].

The problem of optimal location and capacity power of traction sub- stations in this paper, from the previous paragraph and based on [24], is described as an optimization problem with multiple objective functions, as follows where D_{max_i} is i_{th} peak demand, E_i is i_{th} energy needs, x_k is locations of traction substations and x_c is nominal power of traction substation.

The solution to the multiobjective optimization problem in equation (7) is to find or search for a set of solutions that optimally satisfy all objective functions [25] [26]. The set of optimal solutions that can be found is known as the non-dominant solution or Pareto population (optimality) [24].

3. Formulation Optimization with EMO

The EMO optimization method has the peculiarity of being reliable in dealing with complex system problems such as system non-linearity and systems with discrete values [27]. These problems cannot be solved by single-objective function optimization. The difference from single objective function optimization is that in multi-objective function optimization, there are two spaces: a decision space and an objective space. The decision space is the space for independent variables that are satis-ied by the objective function. And the objective space is the result of the objective functions, as shown in figure (2). Where the yellow circles in the decision space are the pareto optimal solutions, they are the pareto optimal fronts in the objective space.

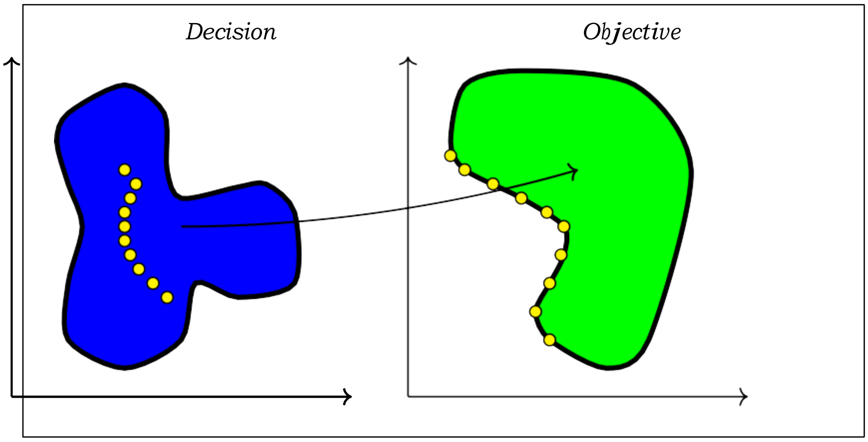

Figure 2. Two space in Multi-objective Optimization [28]

In general, there are two steps to solving EMO optimization: firstly a set of Pareto optimal solutions is found. Secondly, a decision is made from the set of Pareto optimal solutions.

The proposed use of EMO in optimizing the location and capacity of traction substations can be seen in the flowchart in figure (3). It starts with the generation of data from the simulation results of the power requirements of the trains, the position of the trains, and the capacity of the traction substation; this is in the multi-train characteristics block. The multi-train characteristics subroutine block diagram starts with the single-train characteristics equation and rail contour data, train weight, and scheduling. These data are calculated for multiple trains based on the headway and Railway Time Table, resulting in the number of trains and their positions. Then the number of trains and their positions are calculated for the electrical power required, resulting in the characteristics of multiple trains. Then the information from the multi-train block characteristics is given to the block which calculates the power demand and energy needs of each traction substation for each predetermined journey. Then, the objective functions for the power demand and energy needs are given in equation (7). The equation will be used in the next block, the optimization calculation block diagram.

In the optimization block diagram, the search for this non-dominant solution region is done by many algorithms, but in this paper, the NSGA- ii method is used, where the NSGA-ii method [29] has been widely used due to its reliability. The solutions or elements of the decision space in this paper are traction substation location and capacity power. The solutions are sorted into different fronts using a non-dominated fast sorting procedure. Then, at each generation, N descendant solutions are generated from the current population of N solutions. The generated descendant solutions are merged with the current population so that there are (N + N) solutions in the merged population. Then, it is selected as the next population in the following way: First, the non-dominated solution in the merged population is ranked 1 (i.e., the best rank). Second, the solution with rank 1 is removed. Third, the non-dominated solutions are assigned rank 2 among the remaining solutions in the merged population. In this way, all solutions are ranked. Solutions with the same rank are compared using their crowding distance. The same solution evaluation scheme based on non-dominant sorting and crowding distance is also used in binary tournament selection for parent selection for the next generation [28].

After the optimization calculation block is finished, which produces a Pareto optimum for the location of the traction substations and their capacity per generation. The Pareto optimal solutions are forwarded to the higher-level information with the equation (8) block, where the objective function calculation is performed based on the optimal Pareto data generated by the loop.

$$f_{obj} = \alpha_1 \sum_i^{n_{ss}} |x_i - x_{i+1}| + \alpha_2 \sum_i^{n_{ss}} c_i^2 \tag{8}$$

The choice of this final solution will depend heavily on the particular preferences of the human decision-maker. Then, according to the results of the objective function, the optimal traction substation location and capacity power are obtained.

4. Result and Discussion

To find the optimum location and capacity power of DC traction substations, the following data are used: 13 passenger stations, a total distance of about 15 km, and at certain positions on the track there are changes in elevation (table 1) and changes in curvature (table 2).

Table 1. The slope of rail track

No	Position begin (km)	Altitude begin (m)	Position end (km)	Altitude end (m)	Gradient (0/00)
1	8.63	14	10.17	-14	0.0182173
2	12.31	-16.6	13.06	-24	0.0098013
3	13.98	-24	14.96	-18	0.0061038

And assuming that the planned speed of the train is 35 km/h, the maximum speed is 80 km/h, the acceleration is 3.31 km/h, the deceleration is 2.88 km/h, and the delay is 0.15 km/h. And the train set consists of 4 trains with traction motors and 2 trains without traction motors and with 200 passengers per train, where the data are as follows W_m = 191.87 tons, W_t = 89.06 tons, and W_e = 1.1W tons. Where W_m is the weight of four cars with motors, W_t is the weight of two cars without motors, $W = W_m + W_t$ is the total weight of the train set, n is the number of trains, and W_e is the effective weight of 0.8...1.5, which is chosen to be 1.1. And the headway is 10 minutes, and in the morning rush hour for 3 hours. The characteristics of the traction motor are maximum power of 191.5 kW, tractive force of 20.9 kN, and motor efficiency of 0.85. Four trains with motors, where one train has four traction motors, so one train set has 16 traction motors. And the power assumption for auxiliary needs (air conditioning and lighting) is 170 kW. It is assumed that all traction substations are connected, and the calculation of power and energy consumption is performed by sampling the railway power supply system. For multi-objective optimization with GA will using data such as size of population 100, probability of crossover 0.5, probability mutation 0.3, number of generation 10, number point to display from the optimal population 10. The simulator program is *SCILAB*6.1.1 with the solver *optim nsga*2, the others paper already used [30].

Table 2. The slope of rail track

No	Position begin (km)	Position end (km)	Curvature (degree)
1	2.47	2.64	90
2	9.31	9.81	120
3	13.06	13.98	130

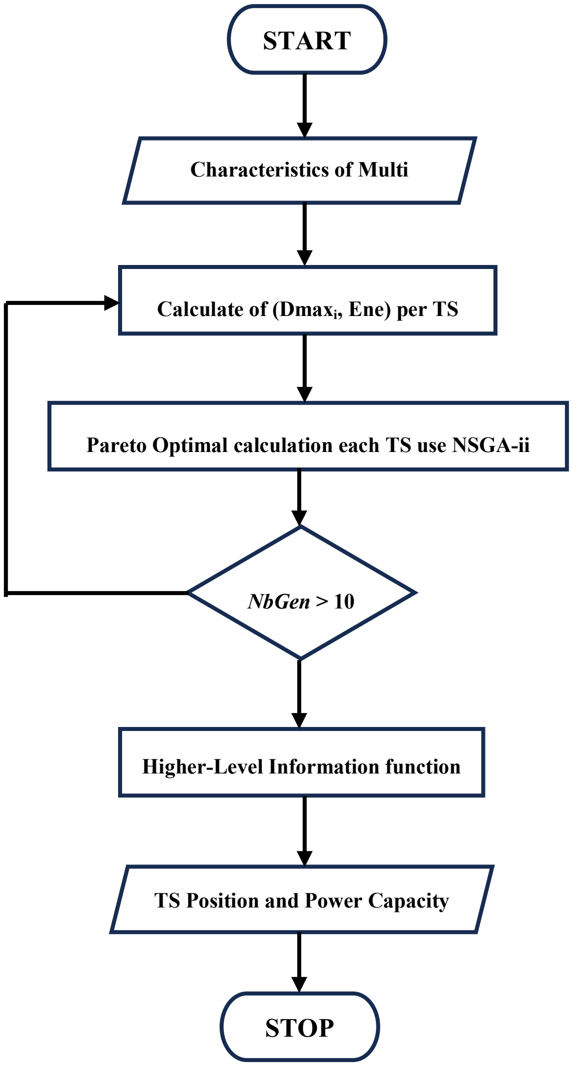

Figure 3. Proposed Algorithm for Location and Capacity Power of DC Traction Substations

Table 3. Specification DC Traction System

No	Item	Specification
1	Catenary Resistance	0.014 ohm/km
2	Rail Resistance	0.0118 ohm/km
3	Substation to earth Resistance	0.5 ohm
4	Rail Conductance	0.00001 mho
5	Substation Rated Voltage	1500 V

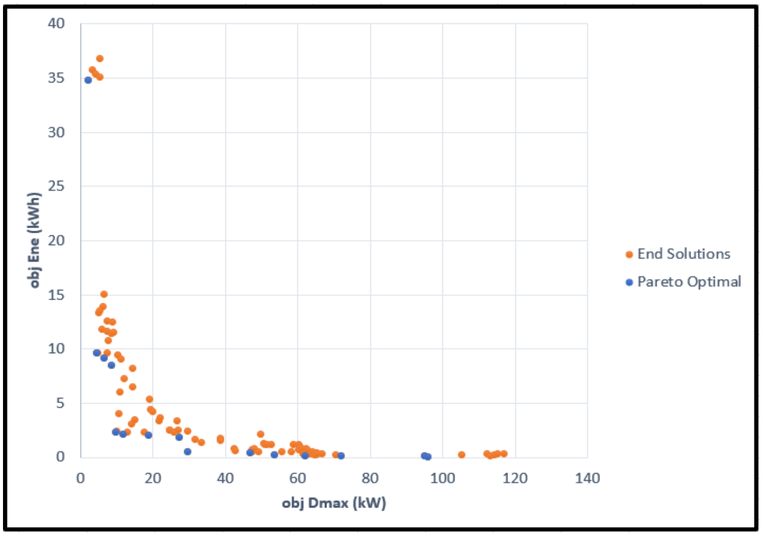

Figure 4. Pareto optimal front for 3 substations with 10 minute headway

The blue nodes in figure(4) or figure(5) are representative of the parameter objectives, obj Dmax and obj Ene, in table (4) or table (5).

Table 4. Pareto optimal solutions for 3 substations with 10 minute headway

SS1 (km)	SS2 (km)	SS3 (km)	Rated Power (kW)	obj Dmax (kW)	obj Ene (kWh)	obj HLI
2.58	7.43	11.78	3267	62.089	0.181	5.337
3.38	6.02	13.33	3188	2.012	34.806	5.081
2.58	7.43	11.76	3280	94.861	0.107	5.380
2.88	7.43	11.88	3122	27.230	1.907	4.874
2.88	7.14	11.70	3115	8.672	8.472	4.852
2.56	7.45	11.76	3277	72.065	0.176	5.371
2.55	7.40	11.81	3243	11.669	2.155	5.249
2.90	7.33	11.88	3122	9.706	2.377	4.874
2.85	7.36	11.83	3122	18.806	2.099	4.874
2.57	7.45	11.80	3230	46.746	0.419	5.217
2.80	6.89	12.12	3301	6.373	9.208	5.449
2.56	7.44	11.75	3283	95.737	0.045	5.390
3.19	7.10	11.96	3199	4.441	9.632	5.117
2.61	7.41	11.82	3260	53.628	0.212	5.313
2.26	7.60	11.78	3306	29.718	0.559	5.466

The pareto optimal solutions for 3 and 4 traction substations are shown in figure(4) and figure(5) with blue nodes. The final population points (yellow points) are dominant solutions near the non-dominate solutions (the pareto optimal front). The result is the 10^{th} generation of multi-objective optimization with NSGA-ii. There are many solutions (the blue points in the figure). The solution found is optimal according to two objective functions in equation (7), both of which minimize the difference in the values of the peak power demand and the energy needs between the traction substations.

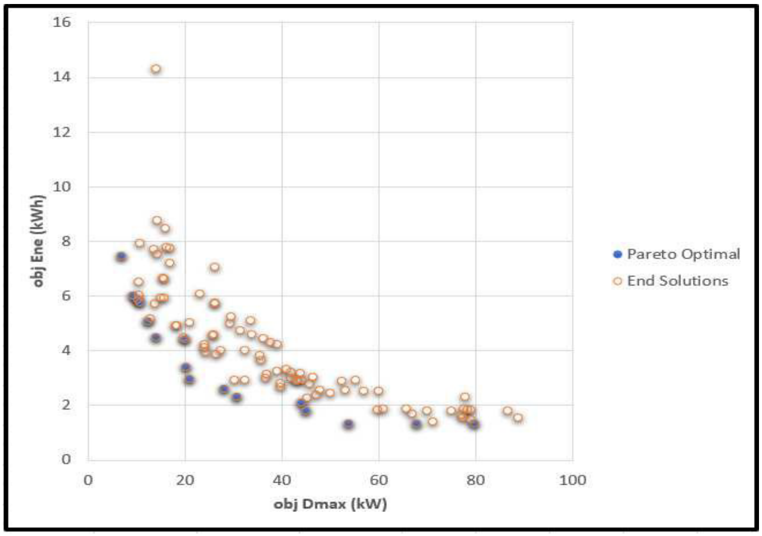

Figure 5. Pareto optimal front for 4 substations with 10 minute headway

Table 5. Pareto optimal solutions for 4 substations with 10 minute headway

SS1 (km)	SS2 (km)	SS3 (km)	SS4 (km)	Rated Power (kW)	obj Dmax (kW)	obj Ene (kWh)	obj HLI
1.60	5.76	9.22	12.34	2340	7.028	7.466	2.7368
2.43	5.50	9.20	12.36	2411	9.445	5.993	2.9061
1.80	5.94	9.34	12.55	2254	67.816	1.325	2.5412
1.68	6.03	9.21	12.32	2261	12.319	5.050	2.5552
1.80	5.89	9.21	12.40	2263	10.279	5.862	2.5605
1.75	6.01	9.33	12.54	2262	53.750	1.326	2.5584
1.72	6.02	9.39	12.43	2270	20.911	2.978	2.5772
1.79	5.94	9.32	12.42	2254	28.145	2.604	2.5391
1.82	5.94	9.32	12.48	2254	44.058	2.103	2.5406
1.80	5.93	9.33	12.54	2254	79.723	1.319	2.5392
1.75	5.95	9.29	12.40	2256	20.294	3.399	2.5457
1.72	6.01	9.34	12.52	2272	30.805	2.323	2.5813
1.77	5.91	9.30	12.37	2263	13.987	4.478	2.5602
1.76	5.91	9.21	12.40	2254	20.048	4.393	2.5407
1.66	6.01	9.21	12.35	2258	10.777	5.759	2.5496
1.82	5.94	9.32	12.50	2254	45.139	1.812	2.5412

From the pareto optimal solution table, a single solution is selected through the higher-level information equation 8 by giving a weight factor with a certain value, where the difference in distance between substations is given a weight factor of one while the average nominal power to the second power is given a weight factor of half. This results in a single solution (cells fully blocked in tables (4) and (5) that is the answer to EMO optimization.

In the case of three traction substations, it is obtained by simulation as follows: the location of the first traction substation is 2.88 km, the second is 7.14 km, and the third is 11.70 km, and the nominal power of the traction substation is 3.115 MW. This satisfies the lowest of equation (8) of 4,852 among other optimal solutions. As for the case of four traction substations, the location of the first traction substation is 1.79 km, the second is 5.94 km, the third is 9.32 km, the fourth is 12.42 km, and the nominal power of the traction substation is 2.254 MW. This result fulfils the lowest of equation (8) of 2.5391 among other optimal solutions.

Then the four traction substations case is compared with the Jakarta MRT data which has 4 traction substations with the positions of the first traction substation 0.377 km, second 4.985 km, third 8.269 km, fourth 13.98 km and the nominal power of the traction substation of 4 MW with a headway of 10 minutes and without considering the energy from regenerative braking, where the value of the result of the function equation (8) is obtained as 21.603.

Some highlights of the simulation results and comparison with data from the Jakarta MRT are:
1. The difference between the simulation results of three traction substations with a nominal power of 3.115 MW and four traction substations with 2.254 MW.
2. the difference of DMax of four traction substations against three trac- tion substations, while ENe of four traction substations is relatively smaller against three traction substations.
3. Compared with the simulation results with EMO optimization of 2.5391, the simulation results are better than the Jakarta MRT data of 21.603.

And the single objective optimization proposed by [9] as a comparative method by using the Jakarta MRT data in the form of the positions of the Traction Substations (0.337 km, 4.985 km, 8.629 km and 13.98 km) assuming a headway of 10 minutes and without considering the energy of regenerative braking the single objective function value of first substation
2.55 km, second substation 6.05 km, third substation 9.54 km, fourth substation 13.26 km, and rated power 4.162 MW is greater than the simulation results with the multi-objective function.

5. Conclusion

The use of the EMO optimization method in finding the optimal loca- tion and capacity Power of the DC traction substation for the rail power system can be carried out. Experiments were carried out on a 15 kilo- meter railway track with three or four traction substations. The load sharing between traction substations is close to the same, or optimal, and minimum nominal power. To achieve optimal conditions, there are two objective functions that must be fulfilled, and the decision variables are the location of the traction substations and the variable capacity of the traction substation. The EMO optimization method is carried out in two steps: finding the Pareto optimal solutions and then using a higher-level information function to determine a single solution among the Pareto optimal solution data.

Future research can expand the case by including regenerative braking factors to determine the location and capacity of the traction box. This requires an algorithm that can change the conductance matrix between trains under regenerative braking or during acceleration. Of course, with fixed assumptions, the traction substation is a rectifier substation that does not have an inverter function.

6. References

[1]. Imran Yusoff, Boon-Kwee Ng, and Suzana Ariff Azizan. Towards sustainable transport policy framework: A rail-based transit system in klang valley, malaysia. *PloS one*, 16(3):e0248519,2021.

[2]. Kathryn G Logan, John D Nelson, Benjamin C McLellan, and Astley Hastings. Electric and hydrogen rail: Potential contribution to net zero in the uk. *Transportation Research Part D: Transport and Environment*, 87:102523, 2020.

[3]. Arturo González-Gil, Roberto Palacin, P Batty, and JP Powell. A systems approach to reduce urban rail energy consumption. *Energy Conversion and Management*, 80:509–524, 2014.

[4]. W.J. Webb. Railway electrification: spacing of substations. *Proceedings of the IEE - Part IA: Electric Railway Traction*, 97:88–92(4), January 1950.

[5]. Laszlo De Koranyi. Design of dc power supply for rapid transit systems. *IEEE Transactions on Industry and General Applications*, IGA-1(2):123–130, 1965.

[6]. Tristan A. Kneschke. Simple method for determination of substation spacing for ac and dc electrification systems. *IEEE Transactions on Industry Applications*, IA-22(4):763–780, 1986.

[7]. S. D. Stoilov. Light rail transit: system design for cost-effectiveness. *Conference on Light Rail Transit*, pages 159–163(5), May 1985.

[8]. D. Gonzalez and F. Manzanedo. Optimal design of a d.c. railway power supply system. In *2008 IEEE Canada ElectricPower Conference*, pages 1–6, 2008.

[9]. Fabio Henrique Pereira, Cassiano Lobo Pires, and Silvio Ikuyo Nabeta. Optimal placement of rectifier substations on dc traction systems. *IET Electrical Systems in Transportation*,4(3):62–69,2014.

[10]. Tahan Lumban Tobing, Tri Desmana Rachmilda, Hilwadi Hindersah, Arwindra Rizqiawan, and Yanuarsyah Haroen. Rectifier substation optimum position on dc traction systems. In *2017 4th International Conference on Electric Vehicular Technology (ICEVT)*, pages 134–138, 2017.

[11]. Umar Sholahuddin, Agus Purwadi, and Yanuarsyah Haroen. Structural optimizations of a 12/8 switched reluctance motor using a genetic algorithm. *International Journal of SustainableTransporta- tion Technology*, 1(1), 2018.

[12]. Maksym Spiryagin Qing Wu and Colin Cole. Longitudinal train dynamics: an overview. *VehicleSystemDynamics*,54(12):1688–1714, 2016.

[13]. Zhongbei Tian, Paul Weston, Ning Zhao, Stuart Hillmansen, Clive Roberts, and Lei Chen. System energy optimisation strategies for metros with regeneration. *TransportationResearch PartC:Emerging Technologies*, 75:120–135, 2017.

[14]. Stuart Hillmansen and Clive Roberts. Energy storage devices in hybrid railway vehicles: A kinematic analysis. *Proceedings of the Institution of Mechanical Engineers, Part F: Journal of Rail and Rapid Transit*, 221(1):135–143, 2007.

[15]. M Chymera and CJ Goodman. The calculation of train performance. In *IET 13th Professional Development Course on Electric Traction Systems*, pages 1–13. IET, 2014.

[16]. Pablo Martínez Fernández, Ignacio Villalba Sanchís, Víctor Yepes, and Ricardo Insa Franco. A review of modelling and optimisation methods applied to railways energy consumption. *Journal of Cleaner Production*, 222:153–162, 2019.

[17]. Caglar Uyulan, Metin Gokasan, and Seta Bogosyan. Modeling, sim- ulation and slip control of a railway vehicle integrated with traction power supply. *Cogent Engineering*, 4(1):1312680, 2017.

[18]. Morris Brenna, Federica Foiadelli, and Dario Zaninelli. *Basic Notions for the Study of Electric Traction Systems*, chapter 2, pages 17–98. John Wiley & Sons Ltd, 2018.

[19]. CJ Goodman, LK Siu, and TK Ho. A review of simulation models for railway systems. In *1998 InternationalConferenceonDevelopments in Mass TransitSystems Conf. Publ. No. 453)*, pages 80–85. IET, 1998.

[20]. Sarosh N Talukdar and Robert L Koo. The analysis of electrified ground transportation networks. *IEEE Transactions on Power Apparatus and Systems*, 96(1):240–247, 1977.

[21]. Yasu Oura, Yoshifumi Mochinaga, and Hiroki Nagasawa. Railway electric power feeding systems. *Japan railway & transport review*, 16(10):48–58, 1998.

[22]. RW Benjamin Stell. Maximum permissible rail potential. *IEEE Vehicular Technology Magazine*, 6(3):99–105, 2011.

[23]. Hadi Saadat. *Power system analysis*. Psa Publishing LLC,2011.

[24]. Carlos A Coello Coello, Gary B Lamont, David A Van Veldhuizen, et al. *Evolutionary algorithmsforsolvingmulti-objectiveproblems*, volume 5. Springer, 2007.

[25]. Sabhan Kanata, Gibson HM Sianipar, Nur Ulfa Maulidevi, et al. Comparison of algorithms to solve multi-objective optimal reactive power dispatch problems in power systems with nonlinear models and a mixture of discrete and continuous variables. *International Journal on ElectricalEngineering & Informatics*, 12(3), 2020.

[26]. Karthik Nagarajan, Ayalur Krishnamoorthy Parvathy, and Arul Rajagopalan. Multi-objective optimal reactive power dispatch using levy interior search algorithm. *Int. J. Electr. Eng. Inform*, 12:547– 570, 2020.

[27]. Kalyanmoy Deb, Amrit Pratap, Sameer Agarwal, and TAMT Meyarivan. A fast and elitist multiobjective genetic algorithm: Nsga-ii. *IEEE transactions on evolutionary computation*, 6(2):182–197, 2002.

[28]. Kalyanmoy Deb. Multi-objective optimization. In *Search methodologies: Introductory tutorials in optimization and decision support techniques*, pages 403–449. Springer, 2013.
[29]. Anulekha Saha, Aniruddha Bhattacharya, Ajoy Kumar Chakraborty, and Priyanath Das. A powerful metaheuristic algorithm to solve static optimal power flow problems: symbiotic organisms search. *International Journal on Electrical Engineering and Informatics*, 10(3):585–614, 2018.
[30]. Petrisor Samoila, Corneliu Cojocaru, Igor Cretescu, Catalina Daniela Stan, Valentin Nica, Liviu Sacarescu, and Valeria Harabagiu. Nanosized spinel ferrites synthesized by sol-gel autocombustion for optimized removal of azo dye from aqueous solution. *Journal of Nanomaterials*, 2015:713802, Jun 2015.

Tahan Lumban Tobing was born in Jakarta, Indonesia in 1971. He grad- uated from University of Indonesia (UI), Indonesia, in 1995 and served as a lecturer in Universitas Kristen Indonesia, Jakarta since 1997. In 2003 he received a M.Sc. degree in Control Engineering from the Karlsruhe Institute of Technology, Karlsruhe, Germany. Since 2016 he is taking a Ph.D. program of the School of Electrical Engineering and Informatics-Institut Teknologi Bandung (ITB). His research interests include Control Engineering, Optimization, and Railway Power Systems. He can be contacted at 33216020@mahasiswa.itb.ac.id and tahan.tobing@uki.ac.id.

Tri Desmana Rachmildha received B.Eng and M.Eng degrees in electrical engineering from Bandung Institute of Technology (ITB), Indonesia, in 1998 and 2002, respectively. He received Doctor Degree in Electrical Engineering from Joint PhD Supervision Program between Institut Nationale Polytechnique de Toulouse, France and School of Electrical Engineering and Informatics, Bandung Institute of Technology, Indonesia, in 2009. He is a researcher at Electrical Energy Conversion Research Laboratory, ITB. Since 2008, he is a lecturer at School of Electrical Engineering and Informatics ITB, Indonesia. His research interests include power electronics and electrical machinery. Dr. Tri Desmana Rachmildha can be contacted trides@konversi.ee.itb.ac.id and trides@gmail.com.

Hilwadi Hindersah graduated his Doctoral program from Institut Teknologi Bandung. His employment as a lecturer and researcher in School of Electrical Engineering and Informatics ITB. His fields of interest are vision-based robot control, interaction design, and adaptive control. He contacted at hilwadi.hindersah@itb.ac.id.

Suwarno graduated in bachelor degree of Electrical Engineering from Ban- dung Institute of Technology (ITB), Indonesia in 1988. He started his master in Electrical Engineering 1989 until 1991 at Bandung Institute of Technology Indonesia (ITB). He graduated his doctoral program at Nagoya University, Japan in 1996. He currently serves as the head of the electric power expertise group at School of Electrical and Informatics, ITB. The focus of his research is related to the science of high voltage and power systems.